Cancer Management and Research

Dovepress

open access to scientific and medical research

Open Access Full Text Article

ORIGINAL RESEARCH

LAPTM4B facilitates tumor growth and induces autophagy in hepatocellular carcinoma

This article was published in the following Dove Press journal:
Cancer Management and Research

Fei Wang[1,2,*]
Huita Wu[3,*]
Sheng Zhang[4,*]
Jing Lu[1]
Yuyan Lu[1]
Ping Zhan[1]
Qinliang Fang[1]
Fuqiang Wang[1]
Xiuming Zhang[5]
Chengrong Xie[1]
Zhenyu Yin[1]

[1]Department of Hepatobiliary Surgery, Fujian Provincial Key Laboratory of Chronic Liver Disease and Hepatocellular Carcinoma, Zhongshan Hospital, Xiamen University, Xiamen, Fujian, People's Republic of China; [2]The United Innovation of Mengchao Hepatobiliary Technology Key Laboratory of Fujian Province, Mengchao Hepatobiliary Hospital of Fujian Medical University, Fuzhou, Fujian, People's Republic of China; [3]Department of Oncology, Zhongshan Hospital, Xiamen University, Xiamen, Fujian, People's Republic of China; [4]Department of Pathology, Hubei Cancer Hospital, Wuhan, Hubei, People's Republic of China; [5]Department of Biomaterials, College of Materials, Xiamen University, Xiamen, Fujian, People's Republic of China

*These authors contributed equally to this work

Correspondence: Chengrong Xie; Zhenyu Yin
Department of Hepatobiliary Surgery, Fujian Provincial Key Laboratory of Chronic Liver Disease and Hepatocellular Carcinoma, Zhongshan Hospital of Xiamen University, 209 South Hubin Road, Xiamen 361004, Fujian Province, People's Republic of China
Email eason_xiecr@126.com; yinzy@xmu.edu.cn

Background: Hepatocellular carcinoma (HCC) is one of the most frequent cancers and the third leading cause of cancer-related deaths. It has been reported that lysosomal associated transmembrane protein LAPTM4B expression is significantly upregulated in human cancers and closely associated with tumor initiation and progression.

Purpose: We aimed to reveal the relevance of LAPTM4B and the pathogenesis of HCC. Methods: Cell viability assessment, colony formation assay, in vivo xenograrft model, microarray, real-time PCR, immunofluorescence and western blot analysis were applied.

Results: Our results demonstrated that LAPTM4B promoted HCC cell proliferation *in vitro* and tumorigenesis *in vivo*. Additionally, upon starvation conditions, LAPTM4B facilitated cell survival, inhibited apoptosis and induced autophagic flux. Expression profiling coupled with gene ontology (GO) analysis revealed that 159 gene downregulated by LAPTM4B silencing was significantly enriched in response to nutrient and some metabolic processes. Moreover, LAPTM4B activated ATG3 transcription to modulate HCC cell apoptosis and autophagy.

Conclusion: Our findings demonstrate that LAPTM4B acts as an oncogene that promotes HCC tumorigenesis and autophagy, and indicate that LAPTM4B may be used as a novel therapeutic target for HCC treatment.

Keywords: autophagy, apoptosis, LAPTM4B, ATG3

Introduction

Hepatocellular carcinoma (HCC) is one of the most frequent cancer diseases and the third leading cause of cancer-related deaths, and its incidence has been steadily rising.[1] HCC typically occurs in patients with chronic liver disease, including non-alcoholic steatohepatitis, alcohol abuse and hepatitis virus infection.[2] Even through the comprehensive treatments for HCC have been greatly improved, the prognoses of HCC patients are still unfavorable, with an approximately 20% 5-year overall survival rate after liver resection.[3] Therefore, revealing the underlying mechanisms of HCC initiation and progression and identifying novel diagnostic and therapeutic biomarkers is urgently needed to improve the prognoses of HCC patients.

The lysosomal-associated transmembrane protein 4B (LAPTM4B) belongs to the membrane-spanning lysosomal LAPTM family of proteins and is an integral lysosomal membrane protein with four transmembrane domains.[4] LAPTM4B expression has been observed to be significantly overexpressed in several human cancers, such as HCC, colorectal cancer, ovarian cancer, and breast cancer.[5,6] Our previous study showed that LAPTM4B expression is upregulated by long noncoding RNA HCAL in HCC.[7] Upregulation of LAPTM4B promotes tumor growth by stimulating the PI3K/Akt pathway and enhances metastasis through activation of MMP2, MMP9 and HIF1α

submit your manuscript | www.dovepress.com
DovePress
http://doi.org/10.2147/CMAR.S201092

expression.[6] In addition, ectopic expression of LAPTM4B facilitates chemotherapy resistance through activation of PI3K/AKT signaling pathway and interacting with multidrug resistance 1 (MDR1).[8]

Autophagy is a conserved lysosome-mediated recycling process that degrades and recycles intracellular components. Autophagy plays important roles in cell survival and maintenance, which enables cancer cells to adapt to stress hypoxia and nutrient starvation conditions.[9] Autophagy-related genes (ATGs) exert crucial functions during autophagy process. For example, ATG3 is essential for vesicle elongation of autophagosome formation. ATG7 mediates the conjugation of ATG12 to ATG5 by association with ATG10, and then induces lipid phosphatidylethanolmine formation.[10] Increasing evidence implies that autophagy play a crucial role in tumorigenesis and cancer progression.[11] Autophagy exerts suppressive effects at the early stage of tumorigenesis, whereas autophagy acts as an oncogene at advanced stages of tumor development.[12] LAPTM4B modulates autophagy during starvation in cancer cells. LAPTM4B knockdown cancer cells cannot undergo autophagosome–lysosome fusion and autolysosome formation in response to the starvation stress.[13] However, the underlying mechanism of LAPTM4B-mediated autophagy and the relationship between LAPTM4B and ATGs has not been determined. In this study, we demonstrated that LAPTM4B promotes HCC tumor growth and autophagy, which is mediated via modulation of ATG3 expression. Our results suggest a key regulator for starvation stress in HCC cells and a potential therapeutic target for HCC treatment.

Materials and methods

Tissue collection

HCC tumor and paired adjacent nontumor tissue samples were obtained from 76 patients who were diagnosed with HCC and underwent liver biopsy between 2012 and 2017 at Zhongshan Hospital of Xiamen University. None of the patients received adjuvant treatment including radiotherapy or chemotherapy before the surgery. Tissue samples were immediately frozen in liquid nitrogen after surgery and stored at -80 °C for further analysis. Written informed consent for research purposes was obtained from all patients. The informed consent and protocols were approved by the ethics committee of the Zhongshan Hospital of Xiamen University. The research has been carried out in accordance with the World Medical Association Declaration of Helsinki.

Cell culture

Two HCC cell lines, PLC/PRF/5 and SMMC-7721, were purchased from the Cell Bank of Chinese Academy of Sciences (China). All cells were routinely cultured in Dulbecco's Modified Eagle Medium DMEM (Hyclone) supplemented with 10% fetal bovine serum (FBS, Biological Industries), 100 U/ml penicillin and 100 g/ml streptomycin in a humidified cell incubator under an atmosphere of 5% CO_2 at 37 °C.

Construction of stable cells

To generate clones stably overexpressing LAPTM4B, PLC/PRF/5 cells were infected with lentiviral particles expressing nothing or human LAPTM4B. Stably clones were selected for 1 week using puromycin and the overexpression efficacy was determined by immunofluorescence and qRT-PCR assays. To generate clones stably silencing LAPTM4B, SMCC-7721 cells were infected with lentiviral particles encoding LAPTM4B shRNA or scramble shRNA control. The target sequence of LAPTM4B shRNA is shown as follow: TACCTGTTTGGTCCTTATTAT. Stably clones were selected for 1 week using puromycin and the knockdown efficacy was determined by immunofluorescence and qRT-PCR assays.

Transfection

shRNA targeting ATG3 (shATG3) was inserted into pLKO.1 vector. The target sequence of ATG3 was shown as follow: GCTACAGGGGAAGAATTGA. Full-length ATG3 was cloned into pLV vector. shATG3 or pLV-ATG3 was transiently transfected into indicated cells using Turbofect (Thermo) according to the manufacturer's instructions. After 48 hrs, the cells were then used for further experiments.

Colony formation

2×10^3 cells were seeded in 6-well dish. After inoculation for 2 weeks, the colonies were fixed with 4% paraformaldehyde, and then stained with 1% crystal violet.

Cell viability detection

HCC cells were seeded at a density of 3×10^3 in 96-well plates. At different time points, cell proliferation and viability was detected by the Cell Counting Kit-8 (CCK-8, Dojindo, Beijing, China) assay as the manufacturer's instructions.

Immunofluorescence (IF)

Cells grown on glass coverslips were fixed with 4% paraformaldehyde for 10 mins. Fixed cells were permeabilized with 0.1% Triton X-100, blocked with PBS containing 1% (w/v) bovine serum albumin for 30 min at room temperature, and incubated with the anti-LC3B (Cell Signaling Technology) or anti-LAPTM4B (Proteintech) antibodies overnight. Staining was visualized with anti-rabbit Alexa Fluor 594 or anti-rabbit Alexa Fluor 488 (Invitrogen) antibodies. After wash, the cells were counterstained with diamidino phenylindole (DAPI) (Sigma) and visualized using a confocal microscope.

RNA isolation and quantitative real-time PCR (qrt-PCR)

Total RNA was isolated using TRIzol Reagent (Invitrogen) according to the standard protocol. RNA was then reverse-transcribed using a GoScript Reverse Transcription Mix (Promega) as the manufacturer's instructions. cDNA was quantified by qRT-PCR using FastStart Universal SYBR Green Master (Roche) in a Lightcycler 96 (Roche) System. GAPDH was used as an internal control. Primers for indicated genes are shown below:

ATG3-Forward: CGGAAGCCGTTAAAGAGATCA, ATG3-Reverse: CTGCAGCTTCTCCTTCATCTT; LAPTM4B-Forward: GGAACTGCTACCGATACATCAA, LAPTM4B-Reverse: TCACAGTGGCATCATCATACG; GAPDH-Forward: CTTTGGTATCGTGGAAGGACTC, GAPDH-Reverse: AGTAGAGGCAGGGATGATGT.

Apoptosis analysis

The cell apoptosis was examined using Apoptosis Detection Kit (Dojindo) as the manufacturer's instructions. In brief, the cells were collected by centrifugation and then treated with Annexin V-FITC and propidium iodide for 15 mins. The cell suspension was immediately analyzed by flow cytometry. The data were analyzed by Kaluza software.

Western blot

Total cell lysates were isolated and fractionated via SDS-PAGE, and separated proteins transferred to PVDF membranes (Millipore). Following blocking in 5% (w/v) nonfat milk, membranes were incubated with the primary antibody and HRP-conjugated secondary antibodies. The signals were detected via chemiluminescence using an ECL Detection Kit (Millipore). The following antibodies were used: anti-LC3B (#3868, Cell Signaling Technology), anti-p62 (#ab91526, Abcam), anti-ACTB (#3700, Cell Signaling Technology).

Microarray detection

Control and LAPTM4B knockdown cells were used for microarray analysis. The mRNA microarray detection was performed by Kangcheng Biotechnology Company (Shanghai, China). Briefly, total RNA from each sample was linearly amplified and labeled with Cy3-UTP. The Labeled cRNAs were purified by RNeasy Mini Kit (Qiagen). The concentration and specific activity of the labeled cRNAs (pmol Cy3/μg cRNA) were measured by NanoDrop ND-1000. 1 μg of each labeled cRNA was fragmented by adding 11 μl 10×Blocking Agent and 2.2 μl of 25×Fragmentation Buffer, then heated at 60°C for 30 min, and finally 55 μl 2×GE Hybridization buffer was added to dilute the labeled cRNA. 100 μl of hybridization solution was dispensed into the gasket slide and assembled to the gene expression microarray slide. The slides were incubated for 17 hrs at 65°C in an Agilent Hybridization Oven. The hybridized arrays were washed, fixed and scanned with using the Agilent DNA Microarray Scanner (part number G2505C). Quantile normalization and subsequent data processing were performed with using Agilent GeneSpring GX v11.5.1 software. A Volcano Plot filtering (Fold Change >2.0, P-value<0.05) between control and LAPTM4B knockdown cells was performed to identify significantly differential expressions of mRNAs. Hierarchical Clustering was performed using the R scripts. GO analysis and Pathway analysis were performed in the standard enrichment computation method.

Animal study

All in vivo animal experiments were approved by the Animal Care and Use Committee of the Xiamen University according to the guidelines followed for the welfare of the animals of the Xiamen University. 5- to 6-week-old male BALB/c nude mice were used to construct xenograft models. 5×10^6 HCC cells with LAPTM4B alteration were injected subcutaneously into the right flanks of the nude mice. After 14 days, tumor growth was detectable and monitored every 3 days. The mice were sacrificed 40 days after inoculation by breaking the neck to death. The tumor tissues were removed and stored at -80°C until used.

Statistical analysis

All statistical analyses were performed using SPSS 18.0 software. Data are shown as mean±SD. The independent

experiments were performed three times. The differences in the results among groups were compared using two-tailed Student's *t*-test or multi-way ANOVA test. Pearson's correlation coefficient was used to measure the linear relationship between the expression levels of LAPTM4B and ATG3 in HCC tissues. All *P*-values less than 0.05 were considered significant.

Results

LAPTM4B facilitates HCC growth in vitro and in vivo

To investigate the functional significance of LAPTM4B in HCC development, we constructed SMMC-7721 cells with stably silenced LAPTM4B expression (Figure 1A). Colony formation and CCK-8 assays showed that knockdown of LAPTM4B expression significantly attenuated the proliferative ability of SMMC-7721 cells (Figure 1B and C). In contrast, we stably overexpressed LAPTM4B in PLC/PRF/5 cells which expressed lower LAPTM4B expression than did in SMMC-7721 cells (Figure 1D). It was found that overexpression of LAPTM4B significantly increased proliferation of PLC/PRF/5 cells compared to that of control cells (Figure 1E and F).

To probe the effect of LAPTM4B on tumorigenesis of HCC cells in vivo, we constructed xenograft models in nude mice. As shown in Figure 1G, tumors grown from LAPTM4B knockdown cells were much smaller than tumors grown from the control cells. Conversely, the growth of tumors from LAPTM4B-upregulated xenografts was significantly increased, compared with that of tumors formed from control xenografts (Figure 1H). These results indicate that LAPTM4B enhances HCC growth in vitro and in vivo.

LAPTM4B enhances HCC cell survival and resistance to apoptosis induced by starvation conditions

The effect of LAPTM4B on cell survival in response to environmental stressor was then examined. Earle's Balanced Salt Solution (EBSS) treatment was used to mimic starvation conditions. It was found that deletion of endogenous LAPTM4B caused a significantly suppression in cell survival (Figure 2A). The LAPTM4B overexpressing PLC/PRF/5 cells exhibited higher cell viability than control cells under starvation conditions (Figure 2B). Furthermore, flow cytometry analysis was performed to examine the role of LAPTM4B in starvation-induced apoptosis. SMMC-7721 cells with LAPTM4B downregulation showed a higher rate of Annexin V-positive cells than did control cells (Figure 2C). In contrast, overexpression of LAPTM4B exerted a protective effect on starvation-induced apoptosis in PLC/PRF/5 cells (Figure 2D). These results indicate that LAPTM4B promotes cell survival and inhibits apoptosis under starvation conditions.

LAPTM4B induces autophagy in HCC cells

Since autophagy play a critical survival role by sustaining viability under starvation conditions, we assessed the effect of LAPTM4B on starvation-induced autophagy in HCC cells. Silencing of LAPTM4B expression could reduce starvation-induced autophagy levels in SMMC-7721 cells, as characterized by a decrease in autophagic marker LC3-II levels and an increase p62 levels (Figure 3A). Conversely, ectopic expression of LAPTM4B significantly induced autophagic flux as evidenced by conversion from LC3B-I to LC3B-II and degradation of p62 in PLC/PRF/5 cells (Figure 3B). To further confirm LAPTM4B on autophagic flux, LC3B puncta formation was detected using immunofluorescence (IF) assays. We observed a significant decrease of LC3B dots accumulation in LAPTM4B-depleted cells (Figure 3C), while the amount of LC3 dots per cell was markedly increased by LAPTM4B overexpression as compared with the control group (Figure 3D). Thus, these results indicate that LAPTM4B promotes autophagy in response to starvation.

LAPTM4B increases ATG3 expression

To gain insight into the molecular mechanisms of LAPTM4B-mediated oncogenic autophagy, microarray analysis was used to compare the transcriptome between control and LAPTM4B knockdown SMMC-7721 cells under starvation condition. As shown in Figure 4A, a wide range of genes expression was altered by depletion of LAPTM4B. Gene ontology (GO) analysis on the 243 genes that were regulated by LAPTM4B silence was performed to explore the functional processes that are affected by LAPTM4B-mediated transcriptional regulation. The 159 genes downregulated by LAPTM4B silencing were significantly enriched in some biological processes, including response to nutrient and some metabolic processes, supporting that LAPTM4B regulated autophagy (Figure 4B). Among these targets of LAPTM4B, ATG3, a critical regulator for autophagy, is of particular interest for its remarkable expression fold change upon LAPTM4B knockdown. qRT-PCR and western blot analysis demonstrated that ATG3

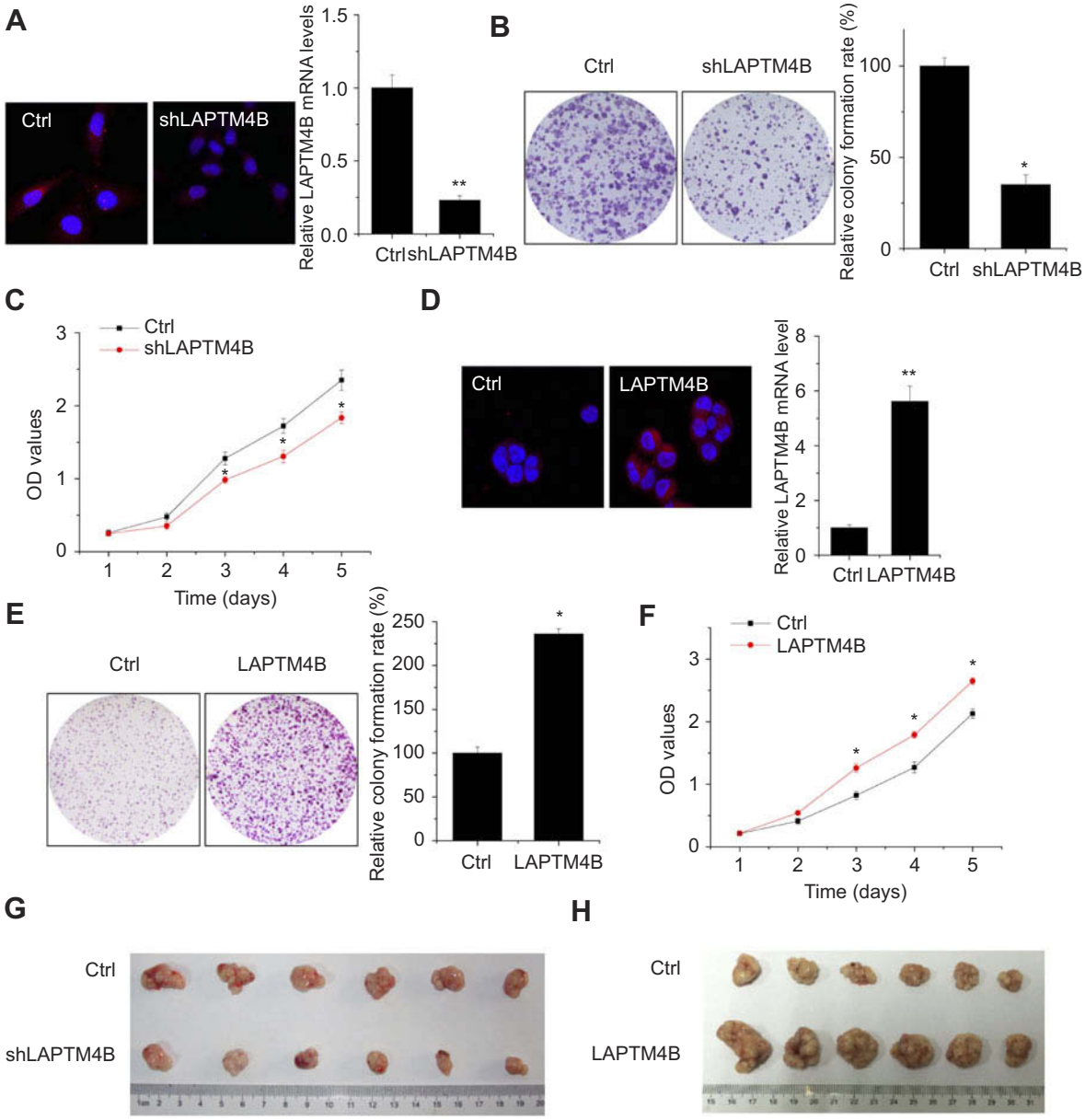

Figure 1 LAPTM4B enhances HCC growth in vitro and in vivo. (**A**) Construction of stably LAPTM4B knockdown SMMC-7721 cells (shLAPTM4B). The knockdown efficacy was determined by IF (left) and qRT-PCR (right). Representative images are shown. (**B**) The colony formation of control and LAPTM4B knockdown SMMC-7721 cells. Representative images are shown. (**C**) The proliferation of control and LAPTM4B knockdown SMMC-7721 cells were detected by CCK-8 assay. (**D**) Construction of stably LAPTM4B overexpressing PLC/PRF/5 cells. The overexpression efficacy was determined by IF (left) and qRT-PCR (right). Representative images are shown. (**E**) The colony formation of control and LAPTM4B overexpressing PLC/PRF/5 cells. Representative images are shown. (**F**) The proliferation of control and LAPTM4B overexpressing PLC/PRF/5 cells was detected by CCK-8 assay. (**G**) SMMC-7721 cells stably expressing LAPTM4B shRNA or the negative control were used for in vivo tumorigenesis. (**H**) PLC/PRF/5 cells stably overexpressing LAPTM4B or the negative control were used for in vivo tumorigenesis. Data are shown as mean ± SD, **P*<0.05, ***P*<0.01.

expression was significantly suppressed by the deletion of LAPTM4B (Figure 4C), whereas ectopic expression of LAPTM4B elevated both mRNA and protein levels of ATG3 (Figure 4D). Consistent with the in vitro results, the expression level of ATG3 markedly decreased in nude mice with LAPTM4B-silencing cells (Figure 4E). Conversely, the LAPTM4B overexpressed group expressed higher ATG3 levels than that did in the control group (Figure 4F).

ATG3 is involved in LAPTM4B-mediated autophagy and survival

To determine whether ATG3 is involved in the LAPTM4B-mediated autophagy and inhibition of apoptosis under starvation, rescue experiments were performed. Upregulation of ATG3 markedly increased LC3B dots accumulation and decreased the number of Annexin V-positive cells in LAPTM4B knockdown cells (Figure S1, Figure 5A and B).

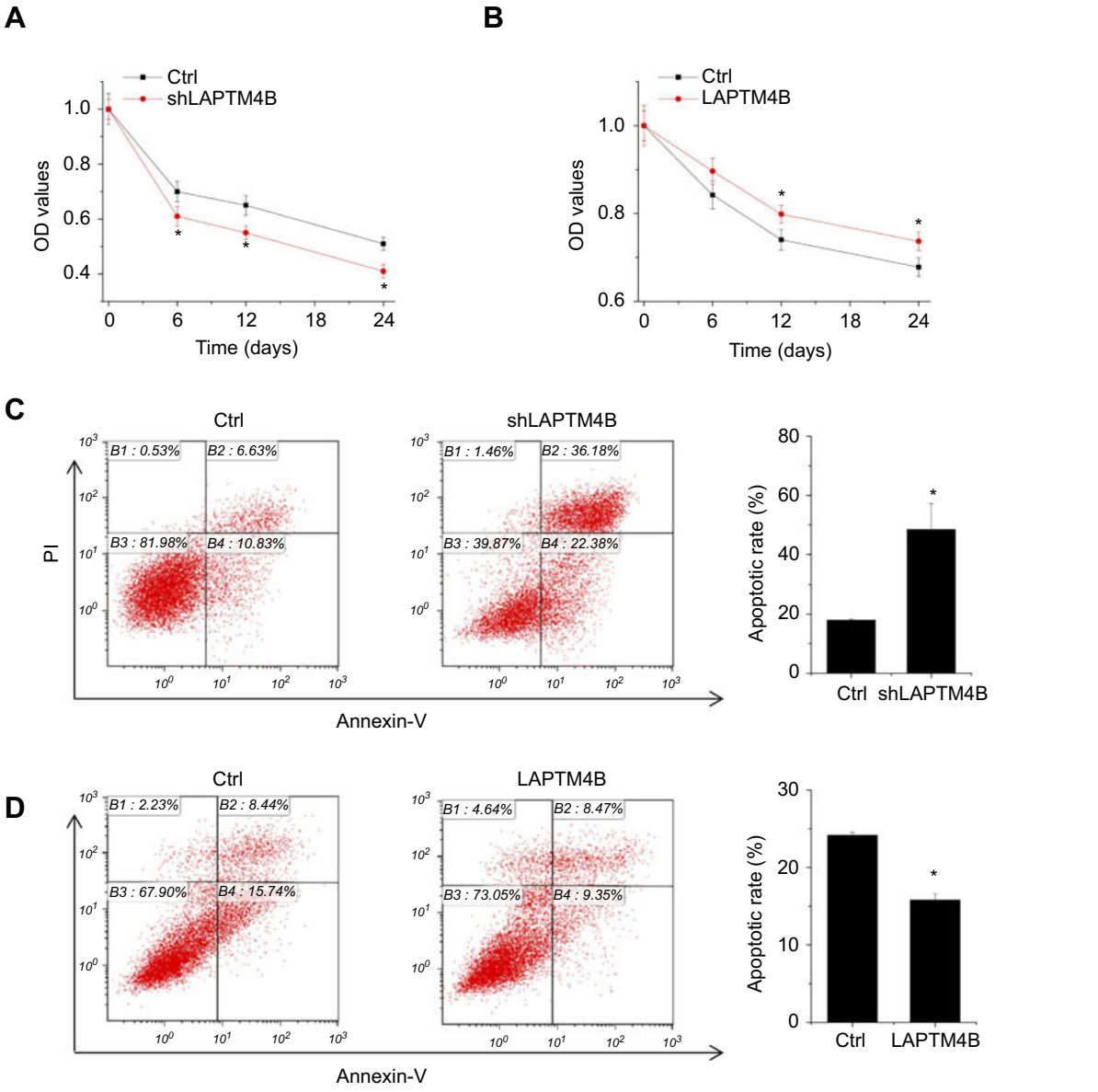

Figure 2 LAPTM4B enhances survival and inhibits apoptosis under starvation conditions. (**A**) Control and LAPTM4B knockdown SMMC-7721 cells were treated with HBSS. At different time point, the cell survival was detected by CCK-8 assay. (**B**) Control and LAPTM4B overexpressing PLC/PRF/5 cells were treated with HBSS. At different time point, the cell survival was detected by CCK-8 assay. (**C**) Control and LAPTM4B knockdown SMMC-7721 cells were treated with HBSS for 24 hrs. The apoptosis was detected by flow cytometry. (**D**) Control and LAPTM4B overexpressing PLC/PRF/5 cells were treated with HBSS for 24 hrs. The apoptosis was detected by flow cytometry. Data are shown as mean ± SD, **P*<0.05.

In contrast, ATG3 knockdown could partly block the LAPTM4B-induced LC3B puncta formation, and promoted apoptosis of LAPTM4B overexpressing cells (Figure S1, Figure 5C and D). These results suggest that ATG3 is responsible for LATPTM4B-mediated autophagy and suppression of apoptosis.

LAPTM4B positively correlates with ATG3 expression in HCC tissues

Because LAPTM4B could upregulate ATG3, we next determined the pathological correlation between LAPTM4B and ATG3 in human HCC samples. The expression levels of LAPTM4B and ATG3 in 76 pairs of HCC and corresponding adjacent noncancerous tissues was detected by qRT-PCR. As shown in Figure 6A and B, both LAPTM4B and ATG3 mRNA levels were higher in HCC tissues than adjacent nontumor liver tissues. Moreover, Pearson correlation analysis showed a positive correlation between LAPTM4B and ATG3 mRNA expression levels in these HCC tissues (r=0.5006, *P*<0.0001, Figure 6C), suggesting an important role of LAPTM4B in modulating ATG3 expression. Additionally, we examined the HCC database

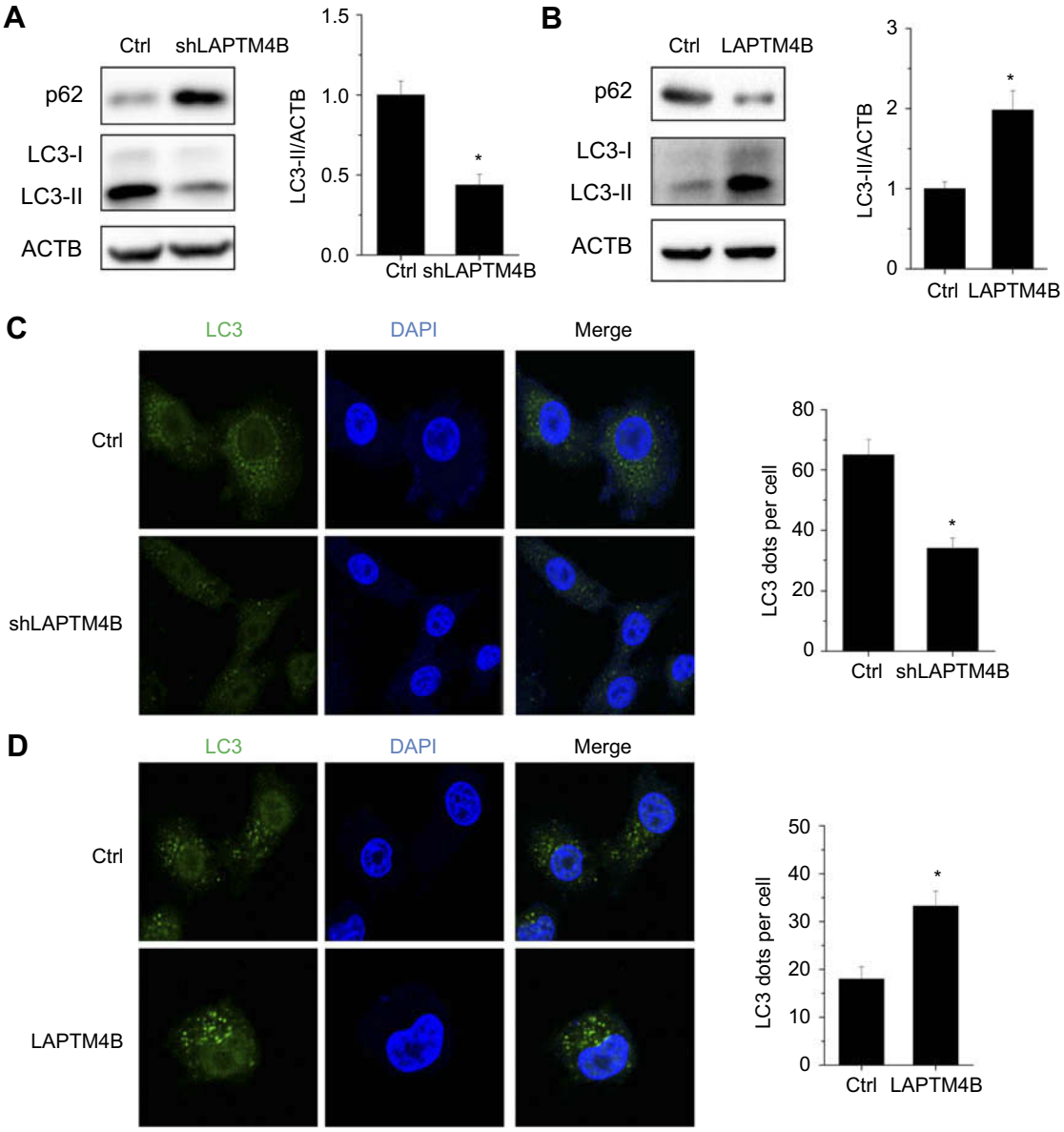

Figure 3 LAPTM4B induces autophagy in HCC cells. (**A**) Evaluation for LC3-Ⅱ and p62 alteration indicative of autophagy induction in control and LAPTM4B knockdown SMMC-7721 cells treated with EBSS for 24 hrs (left). Densitometric analysis normalized to ACTB demonstrating the effect of LAPTM4B silencing on LC3-II levels (right). (**B**) Evaluation for LC3-Ⅱ and p62 alteration indicative of autophagy induction in control and LAPTM4B overexpressing PLC/PRF/5 cells treated with EBSS for 24 hrs (left). Densitometric analysis normalized to ACTB demonstrating the effect of LAPTM4B overexpression on LC3-II levels(right). (**C**) Representative immunofluorescent images showing redistribution of autophagic marker LC3 in LAPTM4B knockdown SMMC-7721 cells treated with EBSS for 24 hrs were taken on a confocal microscope (left). The average number of LC3 dots per cell was counted in more than 5 fields with at least 100 cells for each group (right). Representative images are shown. (**D**) Representative immunofluorescent images showing redistribution of autophagic marker LC3 in LAPTM4B overexpressing PLC/PRF/5 cells treated with EBSS for 24 hrs were taken on a confocal microscope (left). The average number of LC3 dots per cell was counted in more than 5 fields with at least 100 cells for each group (right). Representative images are shown. Data are shown as mean ± SD, *P<0.05.

of The Cancer Genome Atlas (TCGA) to evaluate the differential expression of LAPTM4B and ATG3 between normal and HCC tissues. The results showed that both LAPTM4B and ATG3 were significantly increased in HCC tissues compared to normal tissues by using the UALCAN online analysis (http://ualcan.path.uab.edu/analysis.html) (Figure 6D and E). The Kaplan-Meier analysis showed that HCC with higher expression levels of LAPTM4B or ATG3 was significantly correlated with the elevated rates of mortality (Figure 6F and G).

Discussion

The main finding of our present study was that upon normal conditions, LAPTM4B promotes HCC growth both in vitro and in vivo. Moreover, LAPTM4B enhances cell survival, inhibits apoptosis and induces autophagy in

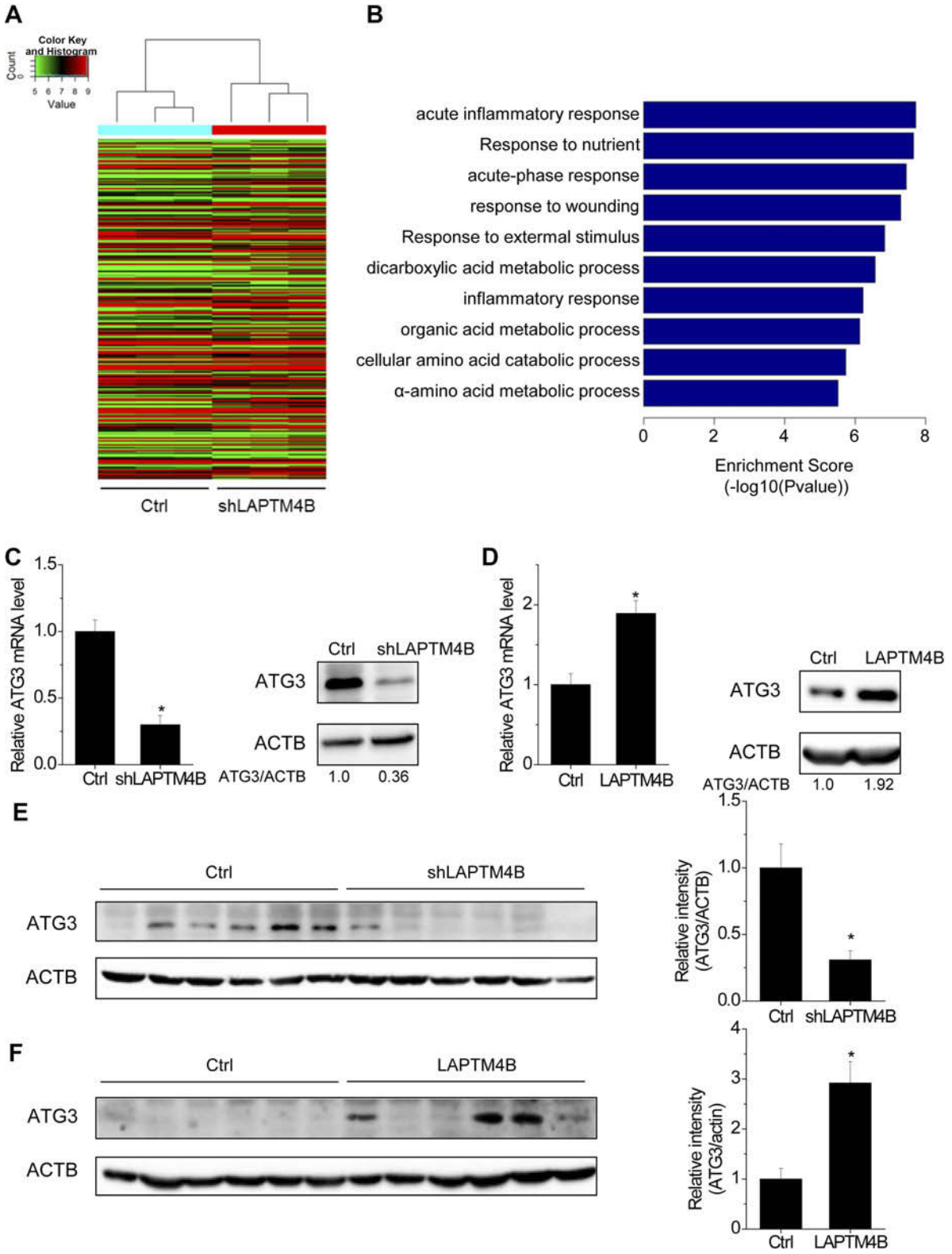

Figure 4 LAPTM4B upregulates ATG3 expression. (**A**) Hierarchically clustered heatmap of upregulated and downregulated genes in control and LAPTM4B knockdown SMMC-7721 cells treated with HBSS for 24 hrs. (**B**) The top 10 biological processes affected by LAPTM4B downregulation by GO. (**C**) The mRNA and protein levels of ATG3 in control and LAPTM4B knockdown SMMC-7721 cells. (**D**) The mRNA and protein levels of ATG3 in control and LAPTM4B overexpressing PLC/PRF/5 cells. (**E**) ATG3 protein levels in the xenografts of nude mice injected with control and LAPTM4B knockdown SMMC-7721 cells were analyzed by performing western blotting (left). Quantification of ATG3 protein levels (right). (**F**) ATG3 protein levels in the xenografts of nude mice injected with control and LAPTM4B overexpressing PLC/PRF/5 cells was analyzed by performing western blotting (left). Quantification of ATG3 protein levels (right). Data are shown as mean ± SD, **P*<0.05.

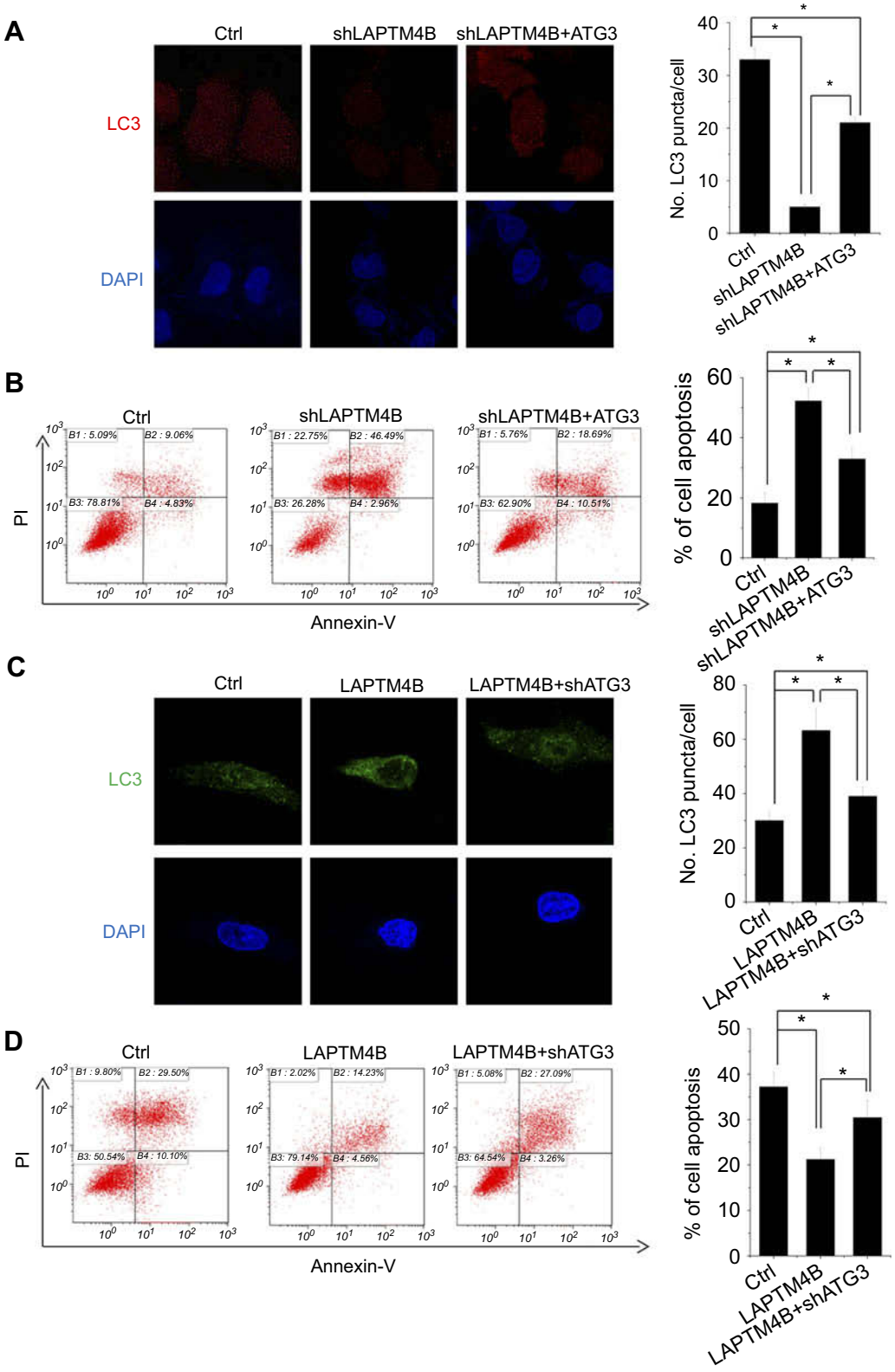

Figure 5 ATG3 takes part in LAPTM4B-mediated autophagy and survival. (**A, B**) The effect of ATG3 overexpression on LC3 accumulation (**A**) and apoptosis (**B**) mediated by LAPTM4B knockdown. (**C, D**) The effect of ATG3 knockdown on LC3 accumulation (**C**) and apoptosis (**D**) mediated by LAPTM4B overexpression. Data are shown as mean ± SD, **P*<0.05.

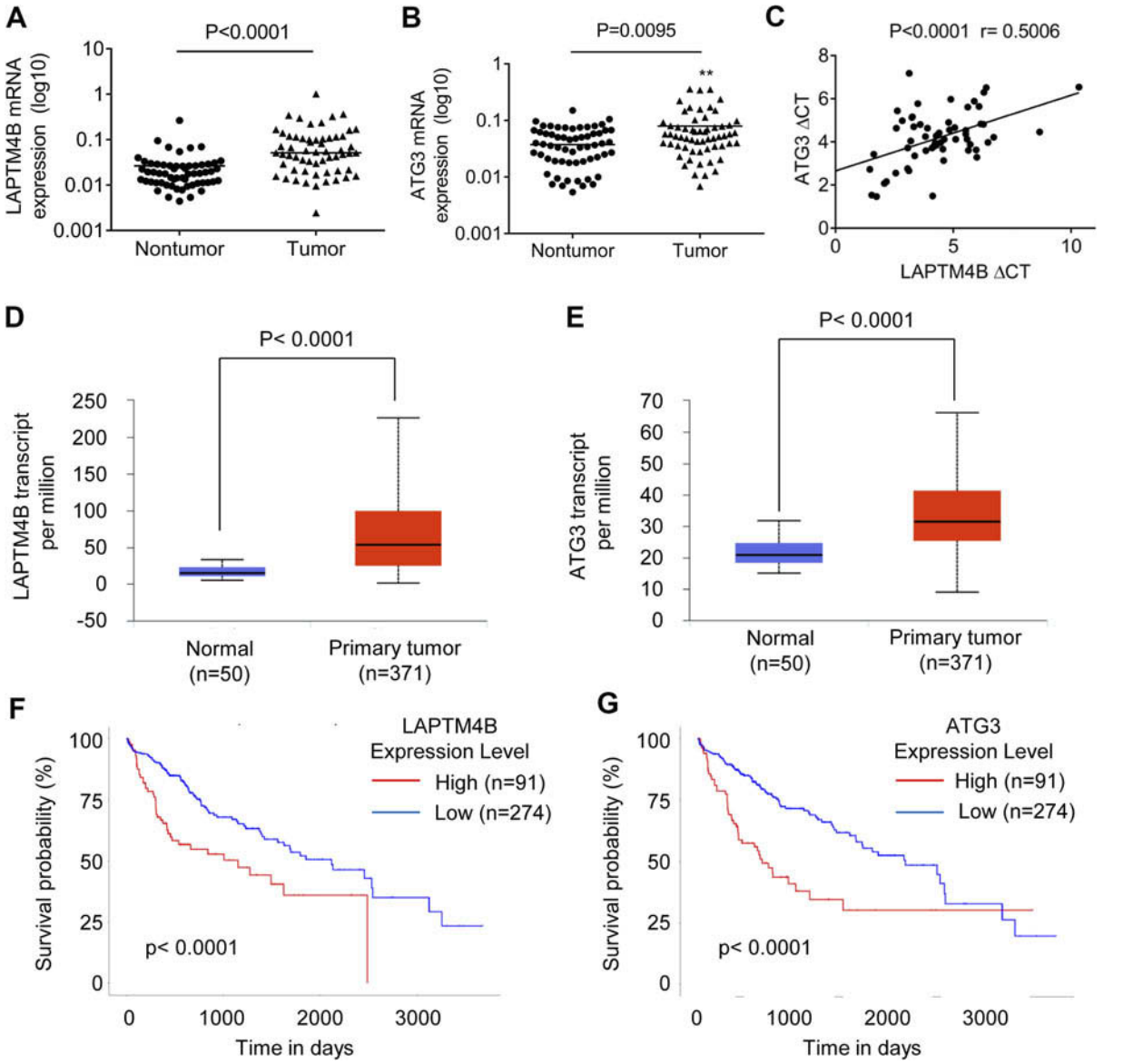

Figure 6 A positive correlation between LAPTM4B and ATG3 expression in HCC tissues. (**A**) The LAPTM4B mRNA levels in 76 pairs of HCC and corresponding adjacent noncancerous tissues were analyzed by qRT-PCR. (**B**) The ATG3 mRNA levels in 76 pairs of HCC and corresponding adjacent noncancerous tissues were analyzed by qRT-PCR. (**C**) The correlation between LAPTM4B and ATG3 mRNA expression in 76 HCC tissues. (**D**) LAPTM4B mRNA expression in normal and HCC tissues from TCGA datasets. Data are mean ± SD. (**E**) ATG3 mRNA expression in normal and HCC tissues from TCGA datasets. Data are mean ± SD. (**F**) Kaplan-Meier survival analysis of the whole HCC patients according to LAPTM4B mRNA expression. The 3rd quatile of LAPTM4B expression in patients was used as a cutoff. High expression patients show expression value >3rd quatile, and low expression patients show expression value <3rd quatile. (**G**) Kaplan-Meier survival analysis of the whole HCC patients according to ATG3 mRNA expression. The 3rd quatile of ATG3 expression in patients was used as a cutoff.

response to starvation through upregulation of ATG3 expression. Hence, our results indicated that LAPTM4B may be considered as a potential therapeutic target for HCC treatment.

LAPTM4B expression is upregulated in a wide range of human cancers due to genetic alteration or abnormal transcriptional regulation. Consistent with previous studies, we also observed a significant increase of LAPTM4B mRNA levels in HCC tissues. *LAPTM4B* gene is mapped to chromosome 8q22.1 where frequently occurs somatic copy number gains in HCC.[14] *LAPTM4B* gene is also one of two genes amplified from chromosome 8q22 which predicts for chemotherapy resistance and recurrence in breast cancer patients.[15] In addition, transcription factors, such as AP4, SP1 and cyclic AMP responsive element-binding protein-1 (CREB1), can bind to the *LAPTM4B* promoter and then upregulate the LAPTM4B transcription.[16–18] Besides, long noncoding RNA and microRNA post-transcriptionally regulates the expression of LAPTM4B.[19] Upregulation of LAPTM4B is

closely associated with the distance metastasis, the differentiation level, and the clinical outcome of patients with cholangiocarcinoma, ovarian cancer, bladder cancer or HCC.[20–23] Together, LAPTM4B may serve as a potential biomarker for the diagnosis and prognostic prediction of patients with cancer. The underlying mechanism of LAPTM4B upregulation in HCC needs further exploration.

Activation of autophagy in cancer cells enhances survival in stressed condition, including nutrient deprivation, hypoxia, and chemotherapy-induced genotoxic damage.[24] LAPTM4B co-localizes with some markers of late endosomes and lysosomes.[25,26] Silence of LAPTM4B increases the lysosomal pH, lysosomal membrane permeabilization, lysosome-mediated cell death and lysosomal release of cathepsins. Under the starvation conditions, deletion of LAPTM4B suppresses autophagosome–lysosome fusion and autolysosome formation in breast cancer cells. In addition, LAPTM4B knockdown promotes autophagosome formation but decreased autophagy flux, indicating that LAPTM4B functinos in later stages of autophagy.[13] A recent study also demonstrated that LAPTM4B exerts functions in epidermal growth factor receptor (EGFR)-related autophagy progression. Upon serum starvation conditions, the interaction of inactive EGFR and LAPTM4B is required for the endosomal accumulation of EGFR. Inactive EGFR and LAPTM4B stabilize each other at endosomes and recruit Sec5, which promotes starvation-induced autophagy.[27] Here, we also showed that LAPTM4B inhibited apoptosis, and enhanced cell survival and autophagy in response to the nutrient deprivation. ATG3 is a key regulator of the autophagy process, which is essential for vesicle elongation formation.[28] Our findings showed that ATG3 was involved in LAPTM4B-mediated autophagy. ATG3 transcription was increased by LAPTM4B, but the exact mechanism by which LAPTM4B influenced the ATG3 expression is unknown. Notably, ATG3 could not completely abolish the effect of LAPTM4B on cell survival and autophagy, indicating that other molecular mechanism may take part in this process. A previous study demonstrated that LAPTM4B upregulated the expression of transcription factor NRF2 following serum deprivation, which led to an increased in NRF2 target genes.[29] Supporting this notion, we speculate that LAPTM4B may activate the ATG3 transcription via NRF2. However, the underlying mechanism by which LAPTM4B increases ATG3 expression to promote autophagy needs further investigation. Taken together, these findings support a crucial role for LAPTM4B in autophagy promotion.

Conclusion

In conclusion, our present study showed that LAPTM4B promoted HCC tumor growth both in vitro and in vivo. Moreover, LAPTM4B facilitated survival and autophagy, while inhibited apoptosis under starvation conditions. We also demonstrated that LAPTM4B induced autophagy in an ATG3-dependent manner. Our findings suggest that LAPTM4B may be a potential target for the progression of HCC.

Acknowledgments

This work was supported by the National Natural Science Foundation of China (No. 81672418, 81702351, 81871961, 81702348 and 81572335), the Natural Science Foundation of Fujian (No.2017-2-101, 2018J01389, 2018J01398 and 2014D022), the Research Project of health and family planning (no. 2018-2-64 and 2018-ZQN-84) and the Science and Technology Project of Xiamen (No. 3502Z20164023, 3502Z20164022).

Author contributions

The molecular and animal experiments were finished by Fei Wang, Huita Wu, Sheng Zhang, Jing Lu, Yuyan Lu, Ping Zhan, Qinliang Fang, Fuqiang Wang, Xiuming Zhang. Zhenyu Yin and Chengrong Xie participated in the design of the study; Fei Wang and Jing Lu participated in data analysis and statistical analysis; Chengrong Xie wrote the manuscript. All authors contributed to data analysis, drafting or revising the article, gave final approval of the version to be published, and agree to be accountable for all aspects of the work.

Disclosure

The authors report no conflicts of interest in this work.

References

1. Siegel RL, Miller KD, Jemal A. Cancer statistics, 2018. *CA Cancer J Clin*. 2018;68(1):7–30. doi:10.3322/caac.21442
2. Hoshida Y. Molecular epidemiology of hepatocellular carcinoma. *Clin liver dis*. 2012;1(6):177–179.
3. Lafaro KJ, Demirjian AN, Pawlik TM. Epidemiology of hepatocellular carcinoma. *Surg Oncol Clin N Am*. 2015;24(1):1–17.
4. Liu XR, Zhou RL, Zhang QY, et al. Structure analysis and expressions of a novel tetratransmembrane protein, lysosoma-associated protein transmembrane 4 beta associated with hepatocellular carcinoma. *World J Gastroenterol*. 2004;10(11):1555–1559.
5. Kasper G, Vogel A, Klaman I, et al. The human LAPTM4b transcript is upregulated in various types of solid tumours and seems to play a dual functional role during tumour progression. *Cancer Lett*. 2005;224(1):93–103.

6. Yang H, Xiong F, Wei X, Yang Y, McNutt MA, Zhou R. Overexpression of LAPTM4B-35 promotes growth and metastasis of hepatocellular carcinoma in vitro and in vivo. *Cancer Lett*. 2010;294(2):236–244.
7. Xie CR, Wang F, Zhang S, et al. Long noncoding RNA HCAL facilitates the growth and metastasis of hepatocellular carcinoma by acting as a ceRNA of LAPTM4B. *Mol Ther Nucleic Acids*. 2017;9:440–451.
8. Li L, Wei XH, Pan YP, et al. LAPTM4B: a novel cancer-associated gene motivates multidrug resistance through efflux and activating PI3K/AKT signaling. *Oncogene*. 2010;29(43):5785–5795.
9. White E, Mehnert JM, Chan CS. Autophagy, metabolism, and cancer. *Clin Cancer Res*. 2015;21(22):5037–5046.
10. Xie Z, Klionsky DJ. Autophagosome formation: core machinery and adaptations. *Nat Cell Biol*. 2007;9(10):1102–1109. doi:10.1038/ncb1007-1102
11. Doria A, Gatto M, Punzi L. Autophagy in human health and disease. *N Engl J Med*. 2013;368(19):1845.
12. Yang S, Wang X, Contino G, et al. Pancreatic cancers require autophagy for tumor growth. *Genes Dev*. 2011;25(7):717–729.
13. Li Y, Zhang Q, Tian R, et al. Lysosomal transmembrane protein LAPTM4B promotes autophagy and tolerance to metabolic stress in cancer cells. *Cancer Res*. 2011;71(24):7481–7489.
14. Wang K, Lim HY, Shi S, et al. Genomic landscape of copy number aberrations enables the identification of oncogenic drivers in hepatocellular carcinoma. *Hepatology*. 2013;58(2):706–717.
15. Li Y, Zou L, Li Q, et al. Amplification of LAPTM4B and YWHAZ contributes to chemotherapy resistance and recurrence of breast cancer. *Nat Med*. 2010;16(2):214–218.
16. Zhang M, Xu JJ, Zhou RL, Zhang QY. cAMP responsive element binding protein-1 is a transcription factor of lysosomal-associated protein transmembrane-4 beta in human breast cancer cells. *PLoS One*. 2013;8(2):e57520.
17. Meng Y, Wang L, Chen D, et al. LAPTM4B: an oncogene in various solid tumors and its functions. *Oncogene*. 2016;35(50):6359–6365.
18. Meng Y, Wang L, Xu J, Zhang Q. AP4 positively regulates LAPTM4B to promote hepatocellular carcinoma growth and metastasis, while reducing chemotherapy sensitivity. *Mol Oncol*. 2018;12(3):373–390.
19. Zhang H, Qi S, Zhang T, et al. miR-188-5p inhibits tumour growth and metastasis in prostate cancer by repressing LAPTM4B expression. *Oncotarget*. 2015;6(8):6092–6104.
20. Zhou L, He XD, Yu JC, et al. Overexpression of LAPTM4B promotes growth of gallbladder carcinoma cells in vitro. *Am J Surg*. 2010;199(4):515–521.
21. Zhou L, He XD, Cui QC, et al. Expression of LAPTM4B-35: a novel marker of progression, invasiveness and poor prognosis of extrahepatic cholangiocarcinoma. *Cancer Lett*. 2008;264(2):209–217.
22. Yang H, Xiong FX, Lin M, Yang Y, Nie X, Zhou RL. LAPTM4B-35 overexpression is a risk factor for tumor recurrence and poor prognosis in hepatocellular carcinoma. *J Cancer Res Clin Oncol*. 2010;136(2):275–281.
23. Yang Y, Yang H, McNutt MA, et al. LAPTM4B overexpression is an independent prognostic marker in ovarian carcinoma. *Oncol Rep*. 2008;20(5):1077–1083.
24. Brech A, Ahlquist T, Lothe RA, Stenmark H. Autophagy in tumour suppression and promotion. *Mol Oncol*. 2009;3(4):366–375.
25. Shao GZ, Zhou RL, Zhang QY, et al. Molecular cloning and characterization of LAPTM4B, a novel gene upregulated in hepatocellular carcinoma. *Oncogene*. 2003;22(32):5060–5069.
26. Vergarajauregui S, Martina JA, Puertollano R. LAPTMs regulate lysosomal function and interact with mucolipin 1: new clues for understanding mucolipidosis type IV. *J Cell Sci*. 2011;124(Pt 3):459–468.
27. Tan X, Thapa N, Sun Y, Anderson RA. A kinase-independent role for EGF receptor in autophagy initiation. *Cell*. 2015;160(1–2):145–160.
28. Kroemer G, Marino G, Levine B. Autophagy and the integrated stress response. *Mol Cell*. 2010;40(2):280–293.
29. Maki Y, Fujimoto J, Lang W, et al. LAPTM4B is associated with poor prognosis in NSCLC and promotes the NRF2-mediated stress response pathway in lung cancer cells. *Sci Rep*. 2015;5:13846.

Supplementary material

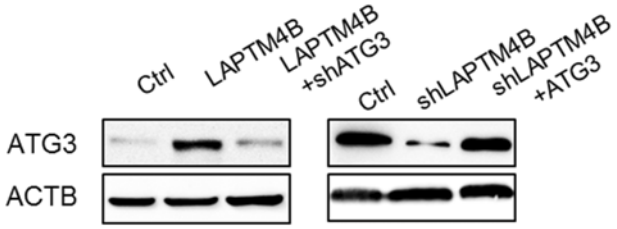

Figure S1 The protein expression of ATG3 in indicated cells.